HHS Public Access

Author manuscript

Neuroscience. Author manuscript; available in PMC 2015 September 28.

Published in final edited form as:

Neuroscience. 2013 January 3; 228: 395–408. doi:10.1016/j.neuroscience.2012.10.035.

Noradrenergic Innervation of Pyramidal Cells in the Rat Basolateral Amygdala

Jingyi Zhang, **Jay F. Muller**, and **Alexander J. McDonald***

Department of Pharmacology, Physiology and Neuroscience, University of South Carolina School of Medicine, Columbia, SC 29208

Abstract

The basolateral nuclear complex of the amygdala (BLC) receives dense noradrenergic (NE) inputs from the locus coeruleus that plays a key role in modulating emotional memory consolidation. Knowledge of the extent of synapse formation by NE inputs to the BLC, as well as the cell types innervated, would contribute to an understanding of how NE modulates the activity of the BLC. To gain a better understanding of NE circuits in the BLC, dual-label immunohistochemistry was used at the light and electron microscopic levels in the present study to analyze NE axons and their innervation of pyramidal cells in the anterior subdivision of the basolateral amygdalar nucleus (BLa). NE axons and BLa pyramidal cells were labeled using antibodies to the norepinephrine transporter (NET) and Ca^{2+}/calmodulin-dependent protein kinase (CaMK), respectively. Dual localization studies using antibodies to NET and dopamine-beta-hydroxylase (DBH) revealed that virtually all NE axons and varicosities expressed both proteins. The BLa exhibited a medium density of NET+ fibers. Ultrastructural analysis of serial section reconstructions of NET+ axons revealed that only about half of NET+ terminals formed synapses. The main postsynaptic targets were small-caliber CaMK+ dendritic shafts and spines of pyramidal cells. A smaller number of NET+ terminals formed synapses with unlabeled cell bodies and dendrites. These findings indicate that the distal dendritic domain of BLa pyramidal cells is the major target of NE terminals in the BLa, and the relatively low synaptic incidence suggests that diffusion from non-synaptic terminals may be important for noradrenergic modulation of the BLa.

Keywords

electron microscopy; immunohistochemistry; norepinephrine transporter; Ca^{2+}/calmodulin-dependent protein kinase II; norepinephrine; dopamine beta-hydroxylase

*Correspondence to: Alexander Joseph McDonald, Telephone: 803-216-3511 Fax: 803-216-3524, alexander.mcdonald@uscmed.sc.edu.

INTRODUCTION

The amygdala is critical for emotional memory formation and the generation of appropriate behavioral responses to salient sensory stimuli and emotionally arousing events in the external world (Millan, 2003; Sah et al., 2003; McGaugh, 2004). As a heterogeneous structure, the amygdala is composed of several nuclei and has connections with numerous brain areas. The basolateral amygdalar nuclear complex (BLC) receives a dense noradrenergic input primarily originating from the locus coeruleus (LC) (Asan, 1998), which is heavily involved in stress and stress-related pathologies (Sved et al., 2002). Studies have shown that stressful stimuli such as foot shock induce norepinephrine (NE) release in the rat amygdala (Galvez et al., 1996; Quirarte et al., 1998). Also, human functional magnetic resonance imaging (fMRI) studies show that elevated NE neurotransmission enhances BLC responses to fear signals (Onur et al., 2009). Moreover, a large amount of evidence indicates that the NE system in the BLC is involved in memory modulation by stress (Cahill et al., 1995; Ferry and McGaugh, 1999; McGaugh, 2004; Ferry and McGaugh, 2008; Roozendaal et al., 2009; McIntyre et al., 2002). Therefore, the LC is important for providing information about aversive stimuli to the BLC and generating appropriate responses to stressors, which suggests that the LC-NE circuit in the BLC could be a potential drug target for anxiety disorders.

Although there is abundant behavioral and clinical evidence for the role of NE system of the BLC in stress and anxiety, there is no clear picture about how NE affects the activity of BLC neurons. Previous studies have shown that there are two major cell classes in the BLC, pyramidal neurons and nonpyramidal neurons. Although these cells do not exhibit a laminar or columnar organization, their morphology, synaptology, electrophysiology, and pharmacology are remarkably similar to their counterparts in the cerebral cortex (McDonald, 1982, 1992a,b; Carlsen and Heimer, 1988; Washburn and Moises, 1992; Rainnie et al., 1993; Sah et al., 2003; Muller et al., 2005, 2006, 2007). Thus, pyramidal neurons in the BLC are projection neurons with spiny dendrites that utilize glutamate as an excitatory neurotransmitter, whereas most nonpyramidal neurons are spine-sparse interneurons that utilize GABA as an inhibitory neurotransmitter. Previous studies indicated that BLC neurons can be inhibited or excited by NE afferents from the LC, but in many cases it was difficult to determine whether the recorded neurons were pyramidal cells or interneurons based on their electrophysiological properties (Buffalari and Grace, 2007, 2009; Chen and Sara, 2007). In a recent investigation in which GABAergic interneurons were identified in brain slices of genetically-modified mice, it was found that some interneurons were excited by NE, but others exhibited little or no response (Kaneko et al., 2008). Thus, there is still considerable confusion regarding the differential modulation of distinct neuronal subpopulations in the BLC by NE.

Anatomical knowledge of NE circuits in the BLC should help to clarify the uncertainties of these physiological studies. A previous electron microscopic study using dopamine-β-hydroxylase (DBH) as a marker for NE axons suggested that only 11% of DBH+ terminals in BLC form synapses (Asan, 1998). This suggests that the NE innervation of the BLC may be mainly mediated by non-junctional, diffuse release of NE into the extracellular space (i.e., “volume transmission”). However, a later study indicated that 31% of DBH+ terminals

in the lateral amygdalar nucleus formed synaptic junctions (Farb et al., 2010). The discrepancies in the two studies may be the result of different criteria for synapse identification, the nucleus studied, or differences in tissue fixation that could affect synaptic morphology. Because these studies analyzed single thin sections, rather than serial section reconstruction of synapses, it seems likely that the synaptic incidence may actually be higher than 31%. This is an important issue to resolve for the BLC since “wired” synaptic transmission and volume transmission have distinct functional correlates in terms of specificity and spatiotemporal aspects of neurotransmission (Agnati et al., 1995).

There is also confusion regarding the postsynaptic targets of NE axon terminals in the BLC. Single-label electron microscopic studies found that the main postsynaptic targets of DBH+ terminals were dendritic shafts and spines, but the cell types of origin of these structures could not be determined (Asan, 1998; Farb et al., 2010). Double-labeling studies using GABA as a marker for interneurons suggested that only about 4% of DBH+ terminals formed synapses with interneurons in the BLC (Li et al., 2002). However, another double-labeling study of the BLC reported that about 30% of DBH+ terminals contacted interneurons that exhibited immunoreactivity for choline acetyltransferase (Li et al., 2001). Thus, it is still not clear to what extent NE terminals synapse with pyramidal projection neurons versus interneurons in the nuclei of the BLC.

The purpose of the present study was to determine the synaptic incidence and postsynaptic targets of NE axon terminals in the anterior subdivision of the basolateral nucleus (BLa), the main nucleus responsible for NE-mediated memory consolidation (McGaugh, 2004). An antibody to the norepinephrine transporter protein (NET) was used to label NE axons since a previous study of this nucleus found that visualization of DBH immunoreactivity at the ultrastructural level required immunohistochemical procedures that hindered morphological preservation of neuronal processes and synapses (Asan, 1998). This is the first electron microscopic study of the amygdala to use NET as a marker for noradrenergic axons. An antibody to the alpha subunit of calcium/calmodulin kinase (CaMK) was used to selectively label pyramidal cells (McDonald et al., 2002) in these dual labeling studies. To obtain a more precise estimation of the synaptic incidence of the NE innervations of the BLa, a serial section analysis of NET+ terminals and their contacts was performed.

EXPERIMENTAL PROCEDURES

Tissue preparation

Male Sprague-Dawley rats weighing 250–350g were used in these experiments. Rats were handled in accordance with the principles of laboratory animal care and protocols approved by the University of South Carolina Institutional Animal Care and Use Committee. Brain tissue was prepared as described in previous studies of our lab (Muller et al., 2011). For light microscopy, rats were anesthetized with chloral hydrate (350 mg/kg) and perfused intracardially with phosphate buffered saline (PBS; pH 7.4) containing 1.0% sodium nitrite (50ml) followed by 4% paraformaldehyde in phosphate buffer (PB; pH 7.4) for 20 mins. Then brains were removed and postfixed in the perfusate for three hours. For electron microscopy, rats were anesthetized and perfused intracardially with PBS containing 0.5% sodium nitrite (50ml) followed by 2% paraformaldehyde-3.75% acrolein in PB for 1 min,

followed by 2% paraformaldehyde in PB for 30 mins. Brains were removed, postfixed in 2% paraformaldehyde for 1 hr, and sectioned on a vibratome in the coronal plane at 50 μm.

Light microscopic immunocytochemistry

Single-label localization of NET+ fibers was performed in two rats using a rabbit antibody to NET (1:2000, antibody 43411, obtained from Dr. Randy D. Blakely, Vanderbilt University School of Medicine). All antibodies were diluted in PBS containing 0.4% Triton X-100 and 1% normal goat serum. Sections were incubated in the primary antibody overnight at 4° C and then processed for the avidin-biotin immunoperoxidase technique using a biotinylated goat anti-rabbit secondary antibody (1:500, Jackson Immunoresearch Laboratories, West Grove, PA) and a Vectastain standard ABC kit (Vector laboratories, Burlingame, CA) with nickel-intensified 3,3′-diaminobenzidine 4HCl (DAB, Sigma Chemical Co., St. Louis, MO, USA) as a chromogen to generate a black reaction product (Hancock, 1986). After the reactions, sections were mounted on gelatinized slides, dried overnight, dehydrated in ethanol, cleared in xylene, and coverslipped in Permount (Fisher Scientific, Pittsburgh, PA, USA). Sections were analyzed with a Nikon E600 microscopy system and digital light micrographs were taken with a Micropublisher digital camera.

Confocal microscopic fluorescence immunocytochemistry

Dual localization studies were performed in two rats using the rabbit NET antibody (1:1000; see above) and a mouse monoclonal antibody to dopamine-beta-hydroxylase (DBH; 1:600; catalog #MAB308, EMD Millipore, Billerica, MA), the synthetic enzyme for norepinephrine, to determine the overlapping extent of NET immunoreactivity and DBH immunoreactivity in the BLa. Sections were incubated in PBS containing 0.4% Triton X-100 and 1% normal goat serum at room temperature for two hours, and then incubated overnight at room temperature in a cocktail of the rabbit NET antibody and the mouse monoclonal DBH antibody. After incubation in the primary antibody cocktail, sections were rinsed in PBS and incubated in a cocktail of goat anti-rabbit Alexa-488 and goat anti-mouse Alexa-546 labeled secondary antibodies (1:400; Invitrogen, Grand Island, NY, USA) for 3h at room temperature. All secondary antibodies were highly cross-adsorbed by the manufacturer to ensure specificity for primary antibodies raised in particular species. Sections were then rinsed in PBS and mounted on glass slides using Vectashield mounting medium (Vector Laboratories; Burlingame, CA).

Sections were examined with a Zeiss LSM 510 Meta confocal microscope. Fluorescence of Alexa 488 (green) and Alexa 546 (red) dyes was analyzed using filter configurations for sequential excitation via 488nm and 543nm channels. Control sections were processed with one of the antibodies omitted from the primary antibody cocktail; in all cases only the labeling with the secondary fluorescent antibodies corresponding to the non-omitted primary antibody was observed, and only on the appropriate channel. These results indicated that the secondary antibodies were specific for rabbit or mouse immunoglobulins, and that there was no “crosstalk” between channels (Wouterlood et al., 1998). Digital images were adjusted for brightness and contrast using Photoshop 6.0 software.

Electron microscopic dual-labeling immunocytochemistry

For electron microscopic studies, a sequential dual-labeling immunoperoxidase method was used in three rats to observe the norepinephrine innervation of pyramidal cells in the anterior subdivision of the basolateral amygdala (BLa) (bregma level −2.1 through −3.0) (Paxinos and Watson, 1986). To enhance penetration of the antibodies, sections were either subjected to a freeze-thaw procedure or were incubated with low levels of Triton-X-100 (0.02–0.04%) in the antibody dilutions. For freeze-thaw, sections were crypoprotected in 30% sucrose in PB for 3 hours, followed by three cycles of freezing-thawing over liquid nitrogen to facilitate antibody penetration. Sections were then rinsed in PB and incubated in a blocking solution (PBS containing 3% normal goat serum and 1% BSA) for 30 mins at room temperature. All antibodies were diluted in the blocking solution.

Sections were incubated in the rabbit antibody to NET (1:2000) for 72 hours at 4° C and then processed using a biotinylated goat anti-rabbit second antibody for one hour (1:400; Jackson Immunoresearch Laboratories, West Grove, PA) and a Vectastain standard ABC kit (Vector Laboratories, Burlingame, CA) with DAB as the chromogen. After rinsing, sections were incubated in a avidin/biotin blocking solution (Vector Laboratories, Burlingame, CA). Sections were then incubated overnight at 4° C in mouse anti-CaMK antibody (1:500–600; Sigma) to label pyramidal cells. For CaMK immunoreactivity, sections were processed using a biotinylated goat anti-mouse secondary antibody (1:200–300, Jackson Immunoresearch Laboratories, West Grove, PA) and an Elite ABC kit (Vector Laboratories). CaMK immunoreactivity was then visualized using a Vector-VIP (Very Intense Purple) peroxidase substrate kit (V-VIP, Vector laboratories). The V-VIP chromogen produces a reaction product that appears purple in the light microscope and granular in the electron microscope, and was easily distinguished from the diffuse DAB immunoperoxidase reaction product at the ultrastructural level.

After the immunocytochemical reactions, sections were postfixed in 2% osmium tetroxide in 0.16 M sodium cacodylate buffer (pH 7.4) for 1 hour, dehydrated in graded ethanols and acetone, and then flat embedded in Polybed 812 (Polysciences, Warrington, PA) in slide molds between sheets of Aclar (Ted Pella, Redding, CA). Selected areas of the BLa were remounted onto resin blanks. Thin sections cut at 65 nm thickness were collected on formvar-coated slot grids, stained with uranyl acetate and lead citrate, and examined with a JEOL-200CX electron microscope. Micrographs were taken with an AMT XR40 digital camera system (Advanced Microscopy Techniques, Danvers, MA)

Analysis

Quantitative analyses were performed in the two brains judged to have the best ultrastructural preservation and immunohistochemistry for NET and CaMK. Two 50 μm vibratome sections from each animal were analyzed. Areas in the thin sections with robust presence of both labels were chosen for quantitative analysis. NET+ axon terminals were identified on the basis of exhibiting clusters of synaptic vesicles. In most cases these terminals were enlargements of the axon (i.e., varicosities), but in other cases they were thinner and appeared to correspond to intervaricose portions of the axon. NET+ terminals were followed and fully or partially reconstructed in 3 to 13 serial thin sections. Synapses

were identified using standard criteria: 1) parallel presynaptic and postsynaptic membranes exhibiting membrane thickenings, 2) a synaptic cleft containing dense material, and 3) clustered synaptic vesicles associated with the presynaptic membrane (Peters et al., 1991). Asymmetrical and symmetrical synapses were identified based on the presence or absence, respectively, of a postsynaptic density and on the relative widths of their synaptic clefts. Whereas synaptic clefts of asymmetrical synapses are typically 20 nm wide, symmetrical synapses have a much narrower synaptic cleft that is only about 12 nm wide (Peters et al., 1991). Similar to many GABAergic symmetrical synapses in the cerebral cortex (e.g., Fig. 11-9 of Peters et al., 1991), the postsynaptic densities of many symmetrical synapses formed by NET+ terminals in the BLa were very thin and created the appearance of a thickened postsynaptic membrane, rather than forming a discrete thickening below the postsynaptic membrane. In addition, the postsynaptic densities of NET+ terminals forming asymmetrical synapses were not as prominent as those associated with glutamatergic synapses of the cerebral cortex (see Fig. 5–7 of Peters et al., 1991).

Postsynaptic neuronal profiles receiving synapses from NET+ varicosities were identified as somata, large-caliber dendritic shafts (>1μm), small-caliber dendritic shafts (<1μm), and spines according to established morphological criteria (Peters et al., 1991). Although CaMK is a reliable marker for pyramidal cells and their processes in the BLa, many spines of pyramidal cells do not exhibit CaMK immunoreactivity (McDonald et al., 2002). However, since the results of previous studies suggest that the great majority of spines observed in electron microscopic studies belong to pyramidal cells (Muller et al., 2006), all spines, whether CaMK + or not, were considered to be of pyramidal cell origin. Because some nonpyramidal cells exhibit a few spines (McDonald, 1982), it is likely that a small number of the CaMK-negative spines observed in this study actually belong to nonpyramidal cells.

Antibody specificity

The rabbit polyclonal NET antiserum (antibody #43411 of Schroeter et al., 2000) was raised against amino acids 585-607 of the intracellular carboxy terminus of mouse NET conjugated to keyhole limpet hemocyanin. The specificity of this antibody has been well documented in a previous study (Schroeter et al., 2000) which demonstrated that: (1) in immunoblots of brain it recognizes a single 80-kDa band corresponding to the mature N-glycosylated NET protein, (2) preadsorption with the peptide eliminated staining of tissue sections and immunoblots, and (3) NET antibody labeling was confined to NE neuronal somata (e.g., locus coeruleus), but absent from brainstem epinephrinergic and dopaminergic neurons, (4) destruction of NE neurons by NE-selective toxins eliminated NET staining. Both light and electron microscopic studies have shown colocalization of dopamine beta hydroxylase, a marker for NE neurons, and NET immunoreactivity using this NET antibody (Schroeter et al., 2000; Miner et al., 2003)

The mouse monoclonal antibody to the α-subunit of CaMK (Sigma; cat. #C265; clone 6G9) was raised against purified type II CaMK. The specificity of this antibody, which recognizes both phosphorylated and nonphosphorylated forms of the kinase, has been well documented in previous studies (Erondu and Kennedy, 1985). On Western blots it produces a single line

at 50 kDa. The CaMK antibody is a reliable marker for pyramidal cell perikarya and dendrites in the BLC (McDonald et al., 2002).

The mouse monoclonal antibody to DBH (EMD Millipore; cat. # MAB308; clone 4F10.2) was raised against purified bovine DBH. This antibody labels noradrenergic somata in the locus coeruleus and other noradrenergic brainstem nuclei, and staining was blocked by preincubating the antibody in wells containing sections of adrenal medulla (Howorth et al., 2009). The staining pattern in the amygdala appeared to be identical to that of other DBH antibodies in previous studies (Fallon and Ciofi, 1992; Asan, 1998), and showed colocalization with NET in virtually all axons in our study (see below).

RESULTS

Light microscopic observations

The distribution of NET+ axons in the amygdala closely matched that obtained with antibodies to DBH in previous studies (Fallon and Ciofi, 1992; Asan, 1998). Thus, in the basolateral nuclear complex the NET+ fiber density was moderate to dense in the basolateral nucleus, but less dense in the lateral nucleus (Fig. 1A). Fiber density was moderate in the basomedial and cortical nuclei. The density of fibers in the anterior portions of the medial nucleus matched that of the adjacent cortical and basomedial nuclei, but fewer fibers were seen in caudal portions of the medial nucleus. Few NET+ fibers were seen in the lateral and capsular portions of the central nucleus (Fig. 1A), but the medial subdivision exhibited a moderate density of fibers. Most NET+ axons had varicosities that were 0.4–1.0 μm in diameter (Fig. 1B). Dual localization experiments of NET and DBH revealed that almost all axons were dual-labeled (Fig. 2). However, there were a few varicosities that were DBH-positive and NET-negative, and some intervaricose segments were NET-positive and DBH-negative. Most varicosities exhibited robust imuunoreactivity for both NET and DBH (Fig. 2B, C).

Electron microscopic observations

At the electron microscopic level, NET+ profiles consisted of thin unmyelinated axons and terminals containing synaptic vesicles (Figs. 3–6, 8–10). The peroxidase reaction product was distributed throughout these NET+ profiles, with accumulations near the plasma membrane and the outer membrane of vesicles and mitochondria. NET+ terminals were round or ovoid and ranged in size from 0.16 to 1.3 μm in diameter. They contained closely-packed clear synaptic vesicles of variable size and shape (Figs. 3–6, 8–10). Occasional dense-core vesicles were also seen (Figs. 3B, 6). The morphology of NET+ profiles was consistent with descriptions of DBH+ profiles reported in previous studies of the basolateral amygdala. (Asan, 1998; Li et al., 2001, 2002; Farb et al., 2010).

NET+ terminals formed synapses with both CaMK+ and unlabeled profiles in our dual-labeling preparations, and their postsynaptic targets include somata, large and small caliber dendrites, and spines (Figs. 3–7, Table 1). No direct contact with endothelial cells surrounding blood vessels was observed, but in one case an NET+ terminal formed an apposition with an astrocytic process surrounding a capillary. The synaptic incidence of

NET+ terminals was determined by examining each terminal in 3 to 13 serial thin sections. The average number of serial sections used to reconstruct terminals forming synapses (6.6 ± 2.4, mean ± SD) was virtually identical to that used to reconstruct non-synaptic terminals (6.5 ± 2.3, mean ± SD). Terminals that lacked distinct contours or occurred in too few available sections to identify synapse formation were excluded from the analysis. About half (45/98 or 46%) of NET+ terminals formed synapses. The size of terminals forming synapses ranged from 0.2 – 0.96 μm in diameter, averaging 0.45 ± 0.19 μm (Mean ± SD). Terminals that did not form synapses ranged in size from 0.16 to 1.28 μm in diameter, averaging 0.61 ± 0.25 μm. Both symmetrical and asymmetrical synapses were observed, but symmetrical synapses were more common (38/45 or 84%) (Table 1).

Most (38/45 or 84%) of the synapses were formed with pyramidal cells (CaMK+ structures and spines) (Figs. 3–5; Table 1, Fig. 7). The main postsynaptic targets were large CaMK+ dendritic shafts (8/38 or 21%; Figs. 3C, 3D), small CaMK+ dendritic shafts (15/38 or 39%; Figs. 3A, 3B, 5C) and spines (14/38 or 37%; Figs. 4, 5D). Synapses formed with unlabeled neuronal processes, presumptive interneurons, mainly targeted small dendritic shafts (Fig. 6). In two instances, NET+ axons encapsulated unlabeled axon terminals and their postsynaptic spines (Figs. 8, 9), forming synapses with the spines.

Some NET+ terminals (7/98 or 7.1%) formed appositions with astrocytic processes that sometimes had characteristics of synaptic junctions (Fig. 10). Astrocytic processes were identified based on their irregular contours and paucity of organelles (Peters et al., 1991).

DISCUSSION

This is the first investigation to use NET as a marker for NE axons in the amygdala. The distribution of NET immunoreactivity (NET-ir) closely matched that of tritiated nisoxetine autoradiographic labeling of NET in the amygdala (Hipolide et al., 2005; Smith and Porrino, 2008). Light microscopy demonstrated that NET+ axons in the BLa almost always exhibited co-localization of DBH. Both NET-ir and DBH-ir were concentrated in axonal varicosities and intervaricose segments of axons. At the ultrastructural level both NET+ axonal varicosities and intervaricose segments formed synapses. This is the first NE study of the BLa to use CaMK immunohistochemistry to identify pyramidal cells, and serial section reconstruction analysis to estimate synaptic incidence. About half of all NET+ axon terminals formed synapses, and the main postsynaptic targets were dendritic shafts and spines of pyramidal cells.

Anatomical Considerations

Given the extensive colocalization of NET-ir and DBH-ir seen in our dual labeling studies, it was not surprising that the morphology of the NET+ axons and terminals appeared to be identical to that of DBH+ axons and terminals seen in previous studies of the BLC (Asan, 1998; Li et al., 2001, 2002; Farb et al., 2010). As in our study using NET as a marker for noradrenergic axons, both varicosities and intervaricose segments of DBH+ axons formed synapses (Asan, 1998; Li et al., 2001). In the initial study of the noradrenergic innervation of the BLC, in which the analysis was confined to the basolateral (BL) and basomedial nuclei (BM), it was reported that 11% of DBH+ terminals formed synapses when observed in

single thin sections (Asan, 1998). However, a later study found that 31% of DBH terminals in the lateral nucleus formed synaptic junctions when observed in single thin sections (Farb et al., 2010). It is not clear if the higher synaptic incidence in the latter study was related to better ultrastructural preservation, perhaps due to the use of acrolein in the fixative (Sesack et al., 2006), or whether this represents a variation of synaptic incidence in the different nuclei studied. The higher synaptic incidence in our study of the BLa (46%) is most likely related to the use of serial section reconstructions of NET+ axon terminals. However, only some of the NET+ terminals were completely reconstructed. Because the average number of serial sections used to reconstruct NET+ terminals was 6.5, and the section thickness was 65 nm, the average reconstructed distance was 4.2 μm. Since the average size of NET+ axon terminals was 5.2 μm, some synapses were undoubtedly missed. Moreover, since an unfavorable orientation may hinder the identification of synapses, especially the small symmetrical synapses formed by most NET+ terminals, it seems likely that an even higher percentage of noradrenergic terminals in the BLa may actually form synapses. Nevertheless, using similar techniques, previous studies in our lab using serial section reconstructions have shown that other neuromodulators in the BLa have a much higher synaptic incidence (serotonin: 76%; dopamine: 77%; acetylcholine: 76%) (Muller et al., 2007, 2009, 2012). This suggests that the NE system in the BLa is unique in its greater reliance on non-synaptic release of transmitter into the extracellular space to modulate neuronal activity (termed “volume transmission” by Agnati et al., 1986, 1995).

In all studies of the NE innervation of the BLC, including the present study, very few NE terminals formed synaptic contacts with cell bodies. In the present investigation, 65% of the postsynaptic targets of NET+ axon terminals were dendritic shafts (either CaMK-positive or negative) and 31% were spines. These percentages are similar to the findings of Asan (1998) in the basolateral/basomedial nuclei (dendritic shafts: 80%; spines: 20%) and Farb and coworkers (2010) in the lateral nucleus (dendritic shafts: 70%; spines: 30%), in single-label DBH studies. In these studies the great majority of spines undoubtedly belonged to pyramidal cells (see Experimental Procedures), but the cell type of origin of dendritic shafts could not be ascertained because no cell type-specific markers were employed.

The use of CaMK as a selective marker for BLa pyramidal cells (McDonald et al., 2002) in the present study allowed us to determine that 84% of NET+ synapses were with pyramidal cells (i.e., CaMK+ structures and spines). This percentage is almost identical to the percentage of neurons in the BLa that are pyramidal cells (85%; McDonald, 1992b). Among pyramidal cell structures, the main postsynaptic targets were large-caliber (i.e., proximal) dendritic shafts (21%), small-caliber distal dendritic shafts (39%), and spines (37%). Thus, most NET+ inputs target the distal dendritic domain (distal dendrites and spines) of pyramidal cells.

CaMK-negative structures (mainly small-caliber dendrites) were postsynaptic targets of 16% of NET+ terminals in the BLa. These structures are presumptive nonpyramidal interneurons, although it is possible that some may be pyramidal cell dendrites that did not exhibit CaMK-ir in the thin sections examined (i.e., “false-negatives”). This percentage is almost identical to the percentage of neurons in the BLa that are interneurons (15%; McDonald, 1992b). These findings are not consistent with previous reports that cholinergic interneurons and

GABAergic interneurons constitute 30% and 4%, respectively, of the targets of DBH+ terminals in the basolateral nucleus (Li et al., 2001, 2002). The reason for this discrepancy is not obvious, but the very high percentage of contacts with dendrites of cholinergic interneurons, which are few in number in the BLC (Carlsen and Heimer, 1986; Nitecka and Frotscher, 1989), suggests the possibility of some false-positive labeling of dendrites.

Both symmetrical and asymmetrical synapses were found in our preparations, but the great majority (84%) of NET+ terminals formed symmetrical synapses with both labeled and unlabeled structures in the BLa. These results are similar to the findings in the lateral nucleus (70% symmetrical; Farb et al., 2010) and BL/BM (70% symmetrical; Asan, 1998) in previous studies. Although symmetrical synapses are typically inhibitory, whereas asymmetrical synapses are excitatory (Shepherd, 2004), this general rule does not appear to hold for all neurotransmitters, especially monoamines and acetylcholine. For example, although acetylcholine has mainly excitatory effects in the BLa, virtually all cholinergic synapses in the BLa are symmetrical (Carlsen and Heimer, 1986; Nitecka and Frotscher, 1989; Muller et al., 2011). It is tempting to speculate that the differences in symmetry of synapses is related to the types of postsynaptic noradrenergic receptor. Thus, anatomical and physiological studies indicate that several different subtypes of alpha adrenergic receptors (Talley et al., 1996; Rosin et al., 1996; Day et al., 1997; Ferry et al., 1997; Buffalari and Grace, 2007) and beta adrenergic receptors (Ferry et al., 1997; Buffalari and Grace, 2007; Abraham et al., 2008; Farb et al., 2010) are expressed by BLa neurons.

Two of the NET+ axon terminals in the present study (2/98, 2% of all NET+ terminals) gave off sheet-like extensions that engulfed unlabeled axon terminals and their postsynaptic spines (Fig. 8 and 9). In both cases the NET+ terminal appeared to form a symmetrical synapse with the spine. These unique engulfing NE terminals have not been described in previous studies of the amygdala, but one was seen in the frontal cortex (see Fig. 11 of Seguela et al., 1990). Although it is difficult to speculate on the full functional significance of these structures, such a configuration would seemingly permit the engulfed synapse to be selectively modulated by NE, and would wall off modulation by any other transmitters that are in the extracellular space surrounding the synapse.

Another interesting aspect of NET+ terminals in the BLa is the formation of appositions with astrocytic processes. These NET+ terminals had synaptic vesicles adjacent to the contact, and the contacting plasma membranes were parallel and often contained dense material in the cleft separating them. These contacts have not been described in previous studies of the amygdala, but have been seen in the visual cortex, where the contacted astrocytic processes were immunoreactive for beta adrenergic receptors (Aoki, 1992). It is of interest in this regard that astrocytes in the lateral amygdalar nucleus of the BLC also exhibit immunoreactivity for beta adrenergic receptors (Farb et al., 2010). There is substantial evidence that NE induces glycogenolysis in astrocytes via alpha and beta adrenergic receptors, and that this process is important for mnemonic function (Berridge and Waterhouse, 2003; Gibbs et al., 2008).

Functional implications

The anatomical results of the present study suggest that NE released into the BLa may have different spheres of influence and temporal dynamics depending on whether it is released from non-synaptic or synaptic axon terminals. The finding that only about half of NET+ terminals form synapses in the BLa suggests that NE axons may function partly by non-junctional, diffuse release of NE into the extracellular space. This intercellular communication mode, called volume transmission (VT), was first introduced by Agnati and Fuxe (Agnati et al., 1986). Unlike traditional junctional or wired transmission (WT), VT lacks any wire-like channel connecting signal source and targets. VT may utilize the same set of neurotransmitters and receptors as WT, but VT signals can be released from axons without synaptic membrane specialization, and they could diffuse in the extracellular space for a long distance (Agnati et al., 2010). VT is principally responsible for the tonic control of brain functions through extrasynaptic receptors, and most CNS drugs, including NET inhibiting antidepressants, primarily affecting neuronal function via VT instead of WT (Vizi et al., 2010).

Although a small number of DBH+ terminals were seen making “possible” synaptic contacts with non-DBH terminals in the lateral nucleus (Farb et al., 2010), it would appear that the main way that NE can modulate transmitter release from axon terminals in the BLa is via VT, after release from non-synaptic terminals or after spillover from synaptic terminals. This explains the ability of NE agonists to potentiate EPSPs in BLa pyramidal cells via β adrenergic receptor enhancement of calcium influx in presynaptic axon terminals of cortical afferents, as well as the reduction of EPSPs via activation of α-2 receptors (Huang et al., 1996, Ferry et al., 1997). There is also evidence that NE release enhances GABA release in the BLa via activation of presynaptic α-1 receptors (Braga et al., 2004).

Stimulation of the locus coeruleus (LC) *in vivo* produces short latency responses in BLa neurons that are most likely due to NE release from terminals forming synapses. The NE released from these terminals could activate adrenergic receptors at the synapse, or perisynaptic receptors near the synapse via transmitter spillover (Agnati et al., 1995; Vizi et al., 2010). Responses were observed in putative pyramidal neurons and interneurons identified based on differences in firing rate, and antidromic activation after stimulation of the cortex (Buffalari and Grace, 2007; Chen and Sara, 2007). Similar responses were observed with iontophoresis of NE directly into the BLa (Buffalari and Grace, 2007). The great majority of BLa neurons were inhibited via activation of α-2 receptors, including all projection neurons antidromically activated by cortical stimulation ((Buffalari and Grace, 2007). These responses clearly correlate with the predominant innervation of CaMK+ pyramidal projection neurons in the present study.

A smaller number of BLa neurons in these *in vivo* studies were excited, and most excitatory responses appeared to be due to activation of β adrenergic receptors (Buffalari and Grace, 2007; Chen and Sara, 2007). Chen and Sara (2007) suggested that the excited neurons were interneurons based on their generally higher firing rate. These responses are most likely due to the NE innervation of the CAMK-negative presumptive interneurons seen in the present study, and the innervation of GABA+ interneurons observed by Li et al., (2002). In *in vitro*

slice studies in genetically-modified mice that express green fluorescent protein in GABAergic neurons, Kaneko et al. (2008) reported that a particular subtype of regular-firing GABAergic interneuron in the BLa was excited via α-1 adrenergic receptors. Thus, it appears that NE released from synaptic terminals innervating pyramidal cells or interneurons has a net inhibitory or excitatory effect, respectively, in the BLa.

The present study demonstrated that the main targets of NET+ terminals were the distal dendritic shafts and spines of CaMK+ pyramidal cells in the BLa. This distal dendritic domain is also the main target of excitatory inputs to pyramidal cells arising from cortical, thalamic, and intra-amygdalar sources (Muller et al., 2006), and contains high levels of glutamatergic N-methyl-D-aspartate receptors (NMDARs; Farb et al., 1995; Gracy and Pickel, 1995). These anatomical findings suggest that NE inputs are in a position to regulate excitatory synaptic plasticity, including long-term potentiation (LTP), by modulating NMDAR currents (Rodrigues et al., 2004; Sigurdsson et al., 2007). In addition, we found that some NET+ terminals formed synapses with CaMK-negative presumptive interneurons. These inputs may be important for the ability of NE to enable the induction of LTP by decreasing the excitability of interneurons that inhibit neighboring pyramidal cells (Tully et al., 2007). Several other studies have provided electrophysiological evidence that NE regulates synaptic plasticity in the basolateral amygdala (Gean et al., 1992; Huang et al., 1998; Huang et al., 2000; DeBock et al., 2003; Huang and Kandel, 2007; Abraham et al., 2008). It has also been shown that activation of β adrenergic receptors can enhance excitatory synaptic transmission and plasticity by trafficking small conductance calcium-activated potassium channels (SK channels), which are located along the dendritic shafts and spines of pyramidal cells, away from the surface plasma membrane (Faber et al., 2008). These mechanisms, as well as others yet to be identified, may contribute to the facilitation of emotional memory consolidation by NE in the BLa (Ferry et al., 1999a, 1999b; Ferry and McGaugh, 1999, 2008; Qu et al., 2008).

Acknowledgments

The authors are grateful for the donation of the NET antibody by Dr. Randy Blakely (Vanderbilt University School of Medicine, Nashville, TN). This work was supported by National Institutes of Health Grant R01-DA027305.

References

Abraham PA, Xing G, Zhang L, Yu EZ, Post R, Gamble EH, Li H. Beta1- and beta2-adrenoceptor induced synaptic facilitation in rat basolateral amygdala. Brain Res. 2008; 1209:65–73. [PubMed: 18396264]

Agnati LF, Fuxe K, Zoli M, Ozini I, Toffano G, Ferraguti F. A correlation analysis of the regional distribution of central enkephalin and beta-endorphin immunoreactive terminals and of opiate receptors in adult and old male rats. Evidence for the existence of two main types of communication in the central nervous system: the volume transmission and the wiring transmission. Acta Physiol Scand. 1986; 128:201–207. [PubMed: 3022556]

Agnati LF, Zoli M, Strömberg I, Fuxe K. Intercellular communication in the brain: wiring versus volume transmission. Neuroscience. 1995; 69:711–726. [PubMed: 8596642]

Agnati LF, Guidolin D, Guescini M, Genedani S, Fuxe K. Understanding wiring and volume transmission. Brain Res Rev. 2010; 64:137–159. [PubMed: 20347870]

Aoki C. Beta-adrenergic receptors: astrocytic localization in the adult visual cortex and their relation to catecholamine axon terminals as revealed by electron microscopic immunocytochemistry. J Neurosci. 1992; 12:781–792. [PubMed: 1347560]

Asan E. The catecholaminergic innervation of the rat amygdala. Adv Anat Embryol Cell. 1998; 142:1–118.

Berridge CW, Waterhouse BD. The locus coeruleus-noradrenergic system: modulation of behavioral state and state-dependent cognitive processes. Brain Res Rev. 2003; 42:33–84. [PubMed: 12668290]

Braga MF, Aroniadou-Anderjaska V, Manion ST, Hough CJ, Li H. Stress impairs alpha(1A) adrenoceptor-mediated noradrenergic facilitation of GABAergic transmission in the basolateral amygdala. Neuropsychopharmacology. 2004; 29:45–58. [PubMed: 14532911]

Buffalari DM, Grace AA. Noradrenergic modulation of basolateral amygdala neuronal activity: opposing influences of alpha-2 and beta receptor activation. J Neurosci. 2007; 27:12358–12366. [PubMed: 17989300]

Buffalari DM, Grace AA. Anxiogenic modulation of spontaneous and evoked neuronal activity in the basolateral amygdala. Neuroscience. 2009; 163:1069–1077. [PubMed: 19589368]

Cahill L, Babinsky R, Markowitsch HJ, McGaugh JL. The amygdala and emotional memory. Nature. 1995; 377:295–296. [PubMed: 7566084]

Carlsen J, Heimer L. A correlated light and electron microscopic immunocytochemical study of cholinergic terminals and neurons in the rat amygdaloid body with special emphasis on the basolateral amygdaloid nucleus. J Comp Neurol. 1986; 244:121–136. [PubMed: 3512630]

Carlsen J, Heimer L. The basolateral amygdaloid complex as a cortical-like structure. Brain Res. 1988; 441:377–380. [PubMed: 2451985]

Chen FJ, Sara SJ. Locus coeruleus activation by foot shock or electrical stimulation inhibits amygdala neurons. Neuroscience. 2007; 144:472–481. [PubMed: 17097235]

Day HE, Campeau S, Watson SJ Jr, Akil H. Distribution of alpha 1a-, alpha 1b- and alpha 1d-adrenergic receptor mRNA in the rat brain and spinal cord. J Chem Neuroanat. 1997; 13:115–139. [PubMed: 9285356]

DeBock F, Kurz J, Azad SC, Parsons CG, Hapfelmeier G, Zieglgänsberger W, Rammes G. Alpha2-adrenoreceptor activation inhibits LTP and LTD in the basolateral amygdala: involvement of Gi/o-protein-mediated modulation of Ca2+-channels and inwardly rectifying K+-channels in LTD. Eur J Neurosci. 2003; 17:1411–1424. [PubMed: 12713644]

Erondu NE, Kennedy MB. Regional distribution of type II Ca2/calmodulin-dependent protein kinase in rat brain. J Neurosci. 1985; 5:3270–3277. [PubMed: 4078628]

Faber ES, Delaney AJ, Power JM, Sedlak PL, Crane JW, Sah P. Modulation of SK channel trafficking by beta adrenoceptors enhances excitatory synaptic transmission and plasticity in the amygdala. J Neurosci. 2008; 28:10803–10813. [PubMed: 18945888]

Fallon, JH.; Ciofi, P. Distribution of monoamines within the amygdala. In: Aggleton, JP., editor. The amygdala. New York: Wiley-Liss; 1992. p. 97-114.

Farb CR, Aoki C, Ledoux JE. Differential localization of NMDA and AMPA receptor subunits in the lateral and basal nuclei of the amygdala: a light and electron microscopic study. J Comp Neurol. 1995; 362:86–108. [PubMed: 8576430]

Farb CR, Chang W, Ledoux JE. Ultrastructural characterization of noradrenergic axons and Beta-adrenergic receptors in the lateral nucleus of the amygdala. Frontiers in Behavioral Neuroscience. 2010; 4:162. [PubMed: 21048893]

Ferry B, Magistretti PJ, Pralong E. Noradrenaline modulates glutamate-mediated neurotransmission in the rat basolateral amygdala in vitro. Eur J Neurosci. 1997; 9:1356–1364. [PubMed: 9240393]

Ferry B, Roozendaal B, McGaugh JL. Basolateral amygdala noradrenergic influences on memory storage are mediated by an interaction between beta- and alpha1-adrenoceptors. J Neurosci. 1999a; 19:5119–5123. [PubMed: 10366644]

Ferry B, Roozendaal B, McGaugh JL. Involvement of alpha1-adrenoceptors in the basolateral amygdala in modulation of memory storage. Eur J Pharmacol. 1999b; 372:9–16. [PubMed: 10374709]

Ferry B, McGaugh JL. Clenbuterol administration into the basolateral amygdala post-training enhances retention in an inhibitory avoidance task. Neurobiol Learn Mem. 1999; 72:8–12. [PubMed: 10371711]

Ferry B, McGaugh JL. Involvement of basolateral amygdala alpha2-adrenoceptors in modulating consolidation of inhibitory avoidance memory. Learn Mem. 2008; 15:238–243. [PubMed: 18391184]

Galvez R, Mesches MH, McGaugh JL. Norepinephrine release in the amygdala in response to footshock stimulation. Neurobiol Learn Mem. 1996; 66:253–257. [PubMed: 8946419]

Gean PW, Huang CC, Lin JH, Tsai JJ. Sustained enhancement of NMDA receptor-mediated synaptic potential by isoproterenol in rat amygdalar slices. Brain Res. 1992; 594:331–334. [PubMed: 1360324]

Gibbs ME, Hutchinson D, Hertz L. Astrocytic involvement in learning and memory consolidation. Neurosci Biobehav Rev. 2008; 32:927–944. [PubMed: 18462796]

Gracy KN, Pickel VM. Comparative ultrastructural localization of the NMDAR1 glutamate receptor in the rat basolateral amygdala and bed nucleus of the stria terminalis. J Comp Neurol. 1995; 362:71–85. [PubMed: 8576429]

Hancock MB. Two-color immunoperoxidase staining: visualization of anatomic relationships between immunoreactive neural elements. Am J Anat. 1986; 175:343–352. [PubMed: 2422916]

Hipólide DC, Moreira KM, Barlow KB, Wilson AA, Nobrega JN, Tufik S. Distinct effects of sleep deprivation on binding to norepinephrine and serotonin transporters in rat brain. Prog Neuropsychopharmacol Biol Psychiatry. 2005; 29:297–303. [PubMed: 15694238]

Howorth PW, Teschemacher AG, Pickering AE. Retrograde adenoviral vector targeting of nociresponsive pontospinal noradrenergic neurons in the rat in vivo. J Comp Neurol. 2009; 512:141–157. [PubMed: 19003793]

Huang CC, Hsu KS, Gean PW. Isoproterenol potentiates synaptic transmission primarily by enhancing presynaptic calcium influx via P- and/or Q-type calcium channels in the rat amygdala. J Neurosci. 1996; 16:1026–1033. [PubMed: 8558230]

Huang CC, Lin CH, Gean PW. Potentiation of N-methyl-D-aspartate currents by isoproterenol in the acutely dissociated rat amygdalar neurons. Neurosci Lett. 1998; 253:9–12. [PubMed: 9754792]

Huang YY, Martin KC, Kandel ER. Both protein kinase A and mitogen-activated protein kinase are required in the amygdala for the macromolecular synthesis-dependent late phase of long-term potentiation. J Neurosci. 2000; 20:6317–25. [PubMed: 10964936]

Huang YY, Kandel ER. Low-frequency stimulation induces a pathway-specific late phase of LTP in the amygdala that is mediated by PKA and dependent on protein synthesis. Learn Mem. 2007; 14:497–503. [PubMed: 17626908]

Kaneko K, Tamamaki N, Owada H, Kakizaki T, Kume N, Totsuka M, Yamamoto T, Yawo H, Yagi T, Obata K, Yanagawa Y. Noradrenergic excitation of a subpopulation of GABAergic cells in the basolateral amygdala via both activation of nonselective cationic conductance and suppression of resting K+ conductance: a study using glutamate decarboxylase 67-green fluorescent protein knock-in mice. Neuroscience. 2008; 157:781–797. [PubMed: 18950687]

Li R, Nishijo H, Wang Q, Uwano T, Tamura R, Ohtani O, Ono T. Light and electron microscopic study of cholinergic and noradrenergic elements in the basolateral nucleus of the rat amygdala: evidence for interactions between the two systems. J Comp Neurol. 2001; 439:411–425. [PubMed: 11596063]

Li R, Nishijo H, Ono T, Ohtani Y, Ohtani O. Synapses on GABAergic neurons in the basolateral nucleus of the rat amygdala: double-labeling immunoelectron microscopy. Synapse. 2002; 43:42–50. [PubMed: 11746732]

McDonald AJ. Neurons of the lateral and basolateral amygdaloid nuclei: a Golgi study in the rat. J Comp Neurol. 1982; 212:293–312. [PubMed: 6185547]

McDonald, AJ. Cell types and intrinsic connections of the amygdala. In: Aggleton, JP., editor. The amygdala. New York: Wiley-Liss; 1992a. p. 67-96.

McDonald AJ. Projection neurons of the basolateral amygdala: a correlative Golgi and retrograde tract tracing study. Brain Res Bull. 1992b; 28:179–185. [PubMed: 1375860]

McDonald AJ, Muller JF, Mascagni F. GABAergic innervation of alpha type II calcium/calmodulin-dependent protein kinase immunoreactive pyramidal neurons in the rat basolateral amygdala. J Comp Neurol. 2002; 446:199–218. [PubMed: 11932937]

McGaugh JL. The amygdala modulates the consolidation of memories of emotionally arousing experiences. Ann Review Neurosci. 2004; 27:1–28.

McIntyre CK, Hatfield T, McGaugh JL. Amygdala norepinephrine levels after training predict inhibitory avoidance retention performance in rats. European J Neurosci. 2002; 16:1223–1226. [PubMed: 12405982]

Millan MJ. The neurobiology and control of anxious states. Progress Neurobiol. 2003; 70:83–244.

Miner LH, Schroeter S, Blakely RD, Sesack SR. Ultrastructural localization of the norepinephrine transporter in superficial and deep layers of the rat prelimbic prefrontal cortex and its spatial relationship to probable dopamine terminals. J Comp Neurol. 2003; 466:478–494. [PubMed: 14566944]

Muller JF, Mascagni F, McDonald AJ. Coupled networks of parvalbumin-immunoreactive interneurons in the rat basolateral amygdala. J Neurosci. 2005; 25:7366–7376. [PubMed: 16093387]

Muller JF, Mascagni F, McDonald AJ. Pyramidal cells of the rat basolateral amygdala: synaptology and innervation by parvalbumin-immunoreactive interneurons. J Comp Neurol. 2006; 494:635–650. [PubMed: 16374802]

Muller JF, Mascagni F, McDonald AJ. Serotonin-immunoreactive axon terminals innervate pyramidal cells and interneurons in the rat basolateral amygdala. J Comp Neurol. 2007; 505:314–335. [PubMed: 17879281]

Muller JF, Mascagni F, McDonald AJ. Dopaminergic innervation of pyramidal cells in the rat basolateral amygdala. Brain Struct Funct. 2009; 213:275–288. [PubMed: 18839210]

Muller JF, Mascagni F, McDonald AJ. Cholinergic innervation of pyramidal cells and parvalbumin-immunoreactive interneurons in the rat basolateral amygdala. J Comp Neurol. 2011; 519:790–805. [PubMed: 21246555]

Muller JF, Mascagni F, Zaric V, McDonald AJ. Muscarinic cholinergic receptor m1 in the basolateral amygdala: ultrastructural localization and synaptic relationships to cholinergic axons. J Comp Neurol. 2012 (In Press).

Nitecka L, Frotscher M. Organization and synaptic interconnections of GABAergic and cholinergic elements in the rat amygdaloid nuclei: single- and double-immunolabeling studies. J Comp Neurol. 1989; 279:470–488. [PubMed: 2918082]

Onur OA, Walter H, Schlaepfer TE, Rehme AK, Schmidt C, Keysers C, Maier W, Hurlemann R. Noradrenergic enhancement of amygdala responses to fear. Socl Cogn Affect Neurosci. 2009; 4:119–126.

Paxinos, G.; Watson, C. The rat brain in stereotaxic coordinates. New York: Academic Press; 1986.

Peters, A.; Palay, SL.; Webster, HD. The fine structure of the nervous system. New York: Oxford University Press; 1991.

Qu LL, Guo NN, Li BM. Beta1- and beta2-adrenoceptors in basolateral nucleus of amygdala and their roles in consolidation of fear memory in rats. Hippocampus. 2008; 18:1131–1139. [PubMed: 18680159]

Quirarte GL, Galvez R, Roozendaal B, McGaugh JL. Norepinephrine release in the amygdala in response to footshock and opioid peptidergic drugs. Brain Res. 1998; 808:134–140. [PubMed: 9767150]

Rainnie DG, Asprodini EK, Shinnick-Gallagher P. Intracellular recordings from morphologically identified neurons of the basolateral amygdala. J Neurophysiol. 1993; 69:1350–1361. [PubMed: 8492168]

Rodrigues SM, Schafe GE, LeDoux JE. Molecular mechanisms underlying emotional learning and memory in the lateral amygdala. Neuron. 2004; 44:75–91. [PubMed: 15450161]

Roozendaal B, McEwen BS, Chattarji S. Stress, memory and the amygdala. Nat Rev Neurosci. 2009; 10:423–433. [PubMed: 19469026]

Rosin DL, Talley EM, Lee A, Stornetta RL, Gaylinn BD, Guyenet PG, Lynch KR. Distribution of alpha 2C-adrenergic receptor-like immunoreactivity in the rat central nervous system. J Comp Neurol. 1996; 372:135–65. [PubMed: 8841925]

Sah P, Faber ES, Lopez De Armentia M, Power J. The amygdaloid complex: anatomy and physiology. Physiol Rev. 2003; 83:803–834. [PubMed: 12843409]

Schroeter S, Apparsundaram S, Wiley RG, Miner LH, Sesack SR, Blakely RD. Immunolocalization of the cocaine- and antidepressant-sensitive l-norepinephrine transporter. J Comp Neurol. 2000; 420:211–232. [PubMed: 10753308]

Seguela P, Watkins KC, Geffard M, Descarries L. Noradrenaline axon terminals in adult rat neocortex: an immunocytochemical analysis in serial thin sections. Neuroscience. 1990; 35:249–264. [PubMed: 2116602]

Sesack, SR.; Miner, LH.; Omelchenko, N. Preembedding immunoelectron microscopy: applications for studies of the nervous system. In: Zaborsky, L.; Wouterlood, FG.; Lanciego, JL., editors. Neuroanatomical tract-tracing 3. New York: SpringerScience +Business Media; 2006. p. 6-71.

Shepherd, GM. Introduction to synaptic circuits. In: Shepherd, GM., editor. The synaptic organization of the brain. Oxford: Oxford University Press; 2004. p. 1-38.

Sigurdsson T, Doyere V, Cain CK, LeDoux JE. Long-term potentiation in the amygdala: a cellular mechanism of fear learning and memory. Neuropharmacology. 2007; 52:215–227. [PubMed: 16919687]

Smith HR, Porrino LJ. The comparative distributions of the monoamine transporters in the rodent, monkey, and human amygdala. Brain Struct Funct. 2008; 213:73–91. [PubMed: 18283492]

Sved AF, Cano G, Passerin AM, Rabin BS. The locus coeruleus, Barrington's nucleus, and neural circuits of stress. Physiol Behav. 2002; 77:737–742. [PubMed: 12527028]

Talley EM, Rosin DL, Lee A, Guyenet PG, Lynch KR. Distribution of alpha 2A-adrenergic receptor-like immunoreactivity in the rat central nervous system. J Comp Neurol. 1996; 372:111–134. [PubMed: 8841924]

Tully K, Li Y, Tsvetkov E, Bolshakov VY. Norepinephrine enables the induction of associative long-term potentiation at thalamo-amygdala synapses. Proc Natl Acad Sci U S A. 2007; 104:14146–14150. [PubMed: 17709755]

Vizi ES, Fekete A, Karoly R, Mike A. Non-synaptic receptors and transporters involved in brain functions and targets of drug treatment. Brit J Pharmacol. 2010; 160:785–809. [PubMed: 20136842]

Washburn MS, Moises HC. Electrophysiological and morphological properties of rat basolateral amygdaloid neurons in vitro. J Neurosci. 1992; 12:4066–4079. [PubMed: 1403101]

Wouterlood FG, Van Denderen JC, Blijleven N, Van Minnen J, Hartig W. Two-laser dual-immunofluorescence confocal laser scanning microscopy using Cy2- and Cy5-conjugated secondary antibodies: unequivocal detection of co-localization of neuronal markers. Brain Res Protoc. 1998; 2:149–159.

Research Highlights

- NE axons in BLa were identified using norepinephrine transporter (NET) antisera.
- NET+ axons in the BLa also contained dopamine beta-hydroxylase.
- Only half of NET+ axon terminals formed synapses in the BLa.
- NET+ axon terminals mainly innervated distal dendrites of BLa pyramidal cells.

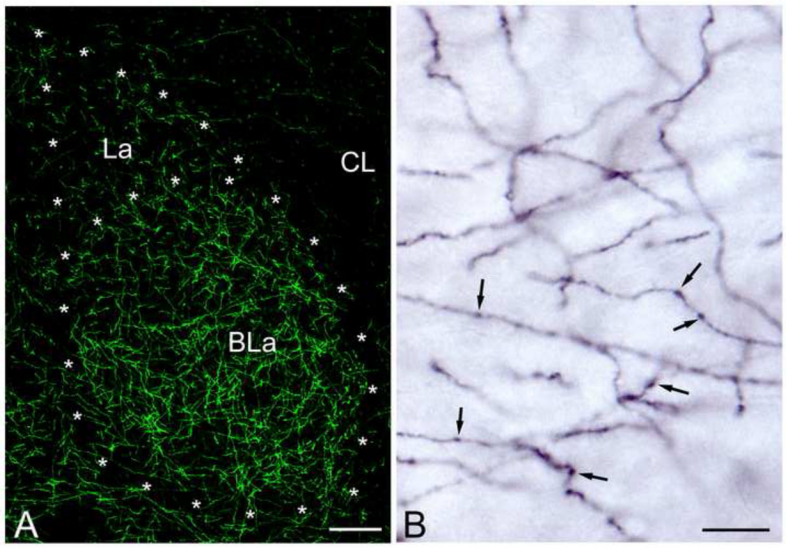

Fig. 1.

NET immunoreactivity in the rat basolateral amygdala. (A) Low power immunofluorescence micrograph illustrating NET+ axons (green) in the BLa, lateral nucleus (La) and lateral subdivision of the central nucleus (CL) at bregma level −2.1. (B) High power micrograph illustrating the morphology of NET+ axons in the BLa using nickel-enhanced DAB as a chromogen in an immunoperoxidase preparation. Arrows point to NET+ varicosities. Scale bars = 100 μm in A, 10 μm in B.

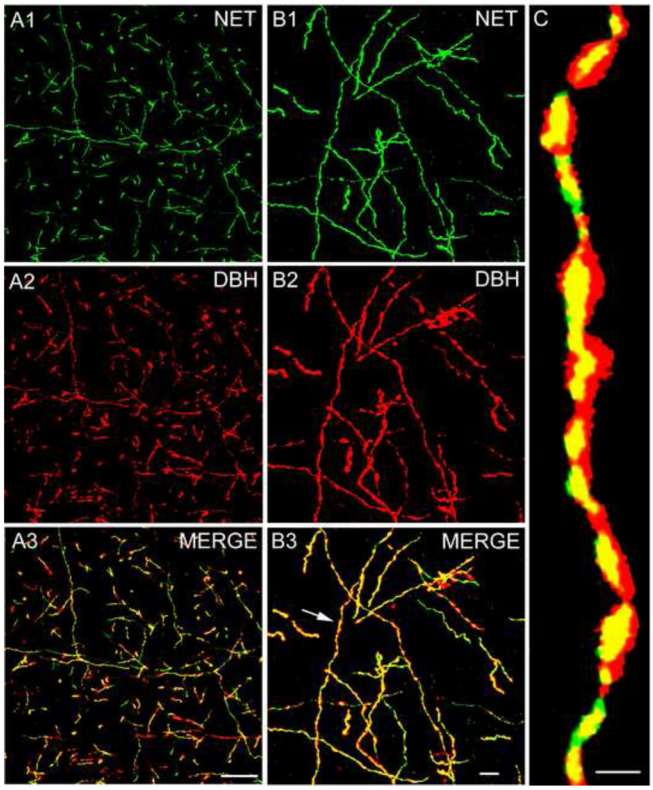

Fig. 2.

NET and DBH immunoreactivity in the rat BLa. (A1–A3) Low power immunofluorescence micrographs showing NET and DBH immunoreactivity in the BLa. (A1) NET+ axons (green) in the BLa. (A2) DBH+ axons (red) in the same field as A. (A3) Merged image showing colocalization of NET and DBH in yellow. Virtually all axons are double-labeled. (B1–B3) Higher magnification Z-series reconstruction of NET and DBH immunoreactivity in the BLa. (B1) NET+ axons (green) in the BLa. (B2) DBH+ axons (red) in the same field as A. (A3) Merged image showing colocalization of NET and DBH in yellow. Virtually all axons are double-labeled. Arrow points to the axonal segment enlarged in C. (C) High power Z-series reconstruction of the axonal segment shown in B3. Double-labeled structures appear yellow. Note extensive colocalization of NET and DBH in axonal varicosites and intervaricose axonal segments. Scale bars = 50 μm in A, 10 μm in B, and 1μm in C.

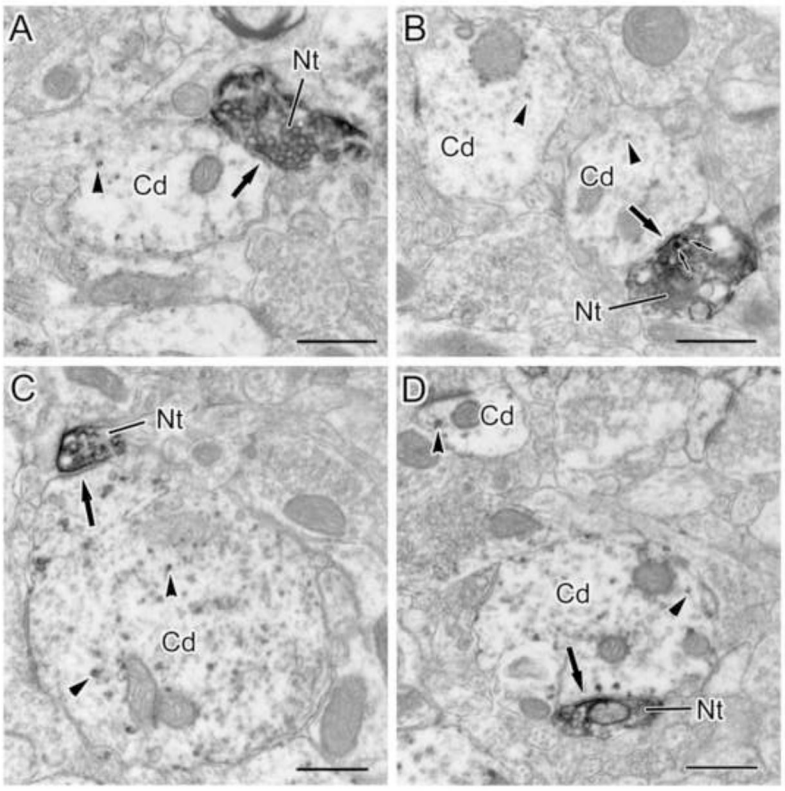

Fig. 3.

NET+ terminals innervate CaMK+ pyramidal cell dendrites in the BLa. (A and B) NET+ terminals (Nt) form symmetrical synapses (arrows) with small-caliber (<1 μm) CaMK+ pyramidal cell dendrites (Cd). The NET+ terminal in B contains two small dense core vesicles (small arrows). The granular V-VIP label for CaMK (arrowheads) is easily distinguished from the diffuse DAB label for NET. (C and D) NET terminals (Nt) form symmetrical synapses (arrows) with large-caliber CaMK+ pyramidal cell dendrites (Cd). Arrowheads indicate particulate V-VIP label for CaMK. Scale bars = 500 nm.

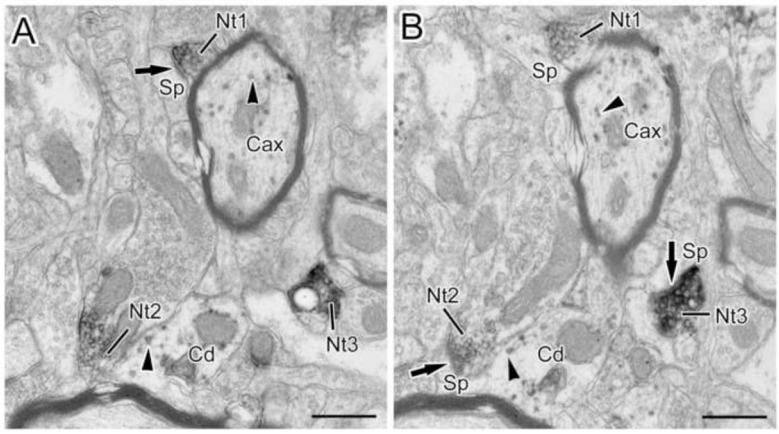

Fig. 4.

(A and B) Two neighboring thin sections in a series through three NET+ terminals (Nt1-3) forming symmetrical (Nt3 in B) and asymmetrical (Nt1 in A and Nt2 in B) synapses (arrows) with spines (Sp). Arrowheads show granules of V-VIP label in a myelinated CaMK + axon (Cax), and a CaMK+ dendrite (Cd). Scale bars = 500 nm.

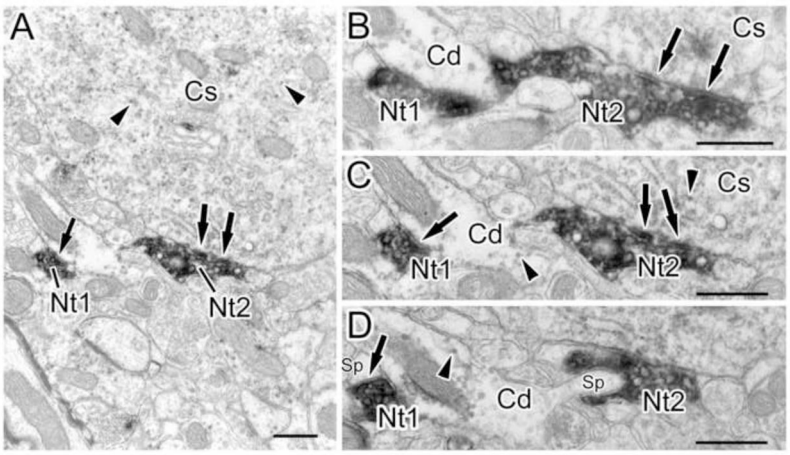

Fig. 5.

An NET+ axon forms multiple synaptic contacts with a CaMK+ pyramidal cell soma and an adjacent CaMK+ dendrite. (A) Low power micrograph showing two terminals (Nt1 and Nt2) of a single NET+ axon forming synaptic contacts (arrows) with a CaMK+ dendritic shaft (left) and a CaMK+ soma (Cs; right). (B–D) Higher power micrographs of three thin sections in a series through the axon shown in A (C corresponds to the section shown in A). (B) Nt2 forms symmetrical synapses (arrows) with a CaMK+ pyramidal cell soma (Cs; also seen in C). (C) Nt1 forms a synapse (arrow) with a CaMK+ dendritic shaft (Cd; arrow on left). This synapse appears symmetrical in this section, but appears to be associated with a postsynaptic density in B. (D) Nt2 surrounds and appears to synapse with a spine (Sp on right) that extends outward from the CaMK+ dendritic shaft (Cd). Nt1 forms a symmetrical synapse with a different spine (Sp on left). Arrowheads show granules of V-VIP label in C and D. B–D are the 12^{th}, 10^{th}, and 8^{th} sections, respectively, from a 12 section series. Scale bars = 500 nm.

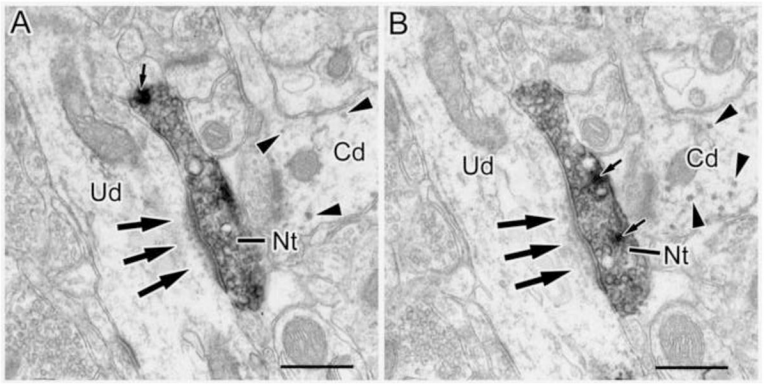

Fig. 6.

(A and B) Two neighboring thin sections in a series through an NET+ terminal (Nt) that forms an asymmetrical synapse (arrows) with an unlabeled dendrite (Ud). Note subsynaptic dense bodies below the postsynaptic density. Arrowheads show granules of V-VIP label in an adjacent CaMK+ dendritic shaft. Small arrows indicate dense core vesicles. Scale bar = 500 nm.

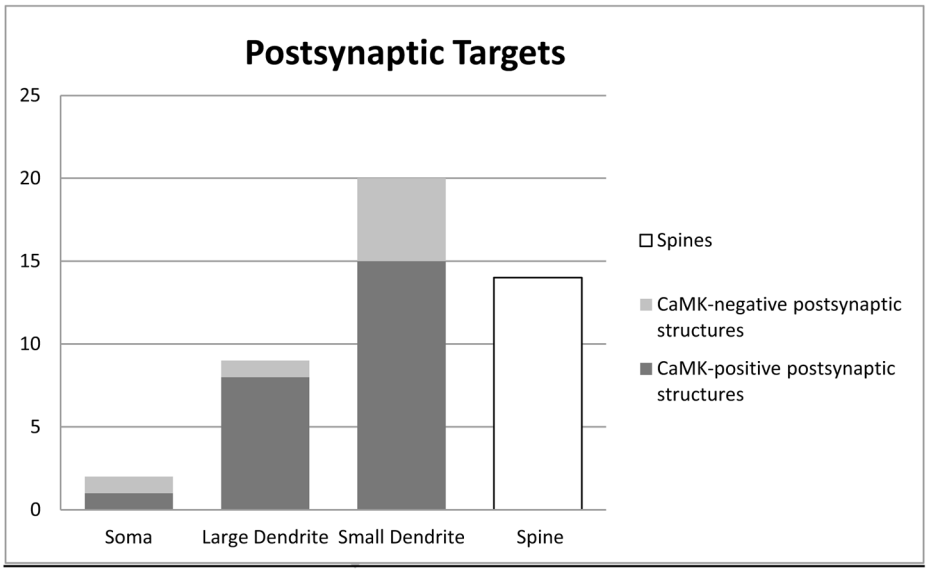

Fig. 7.

Histogram showing the numbers of synapses of NET+ terminals with CaMK-positive (dark gray) or CaMK-negative (light gray) structures and spines (white).

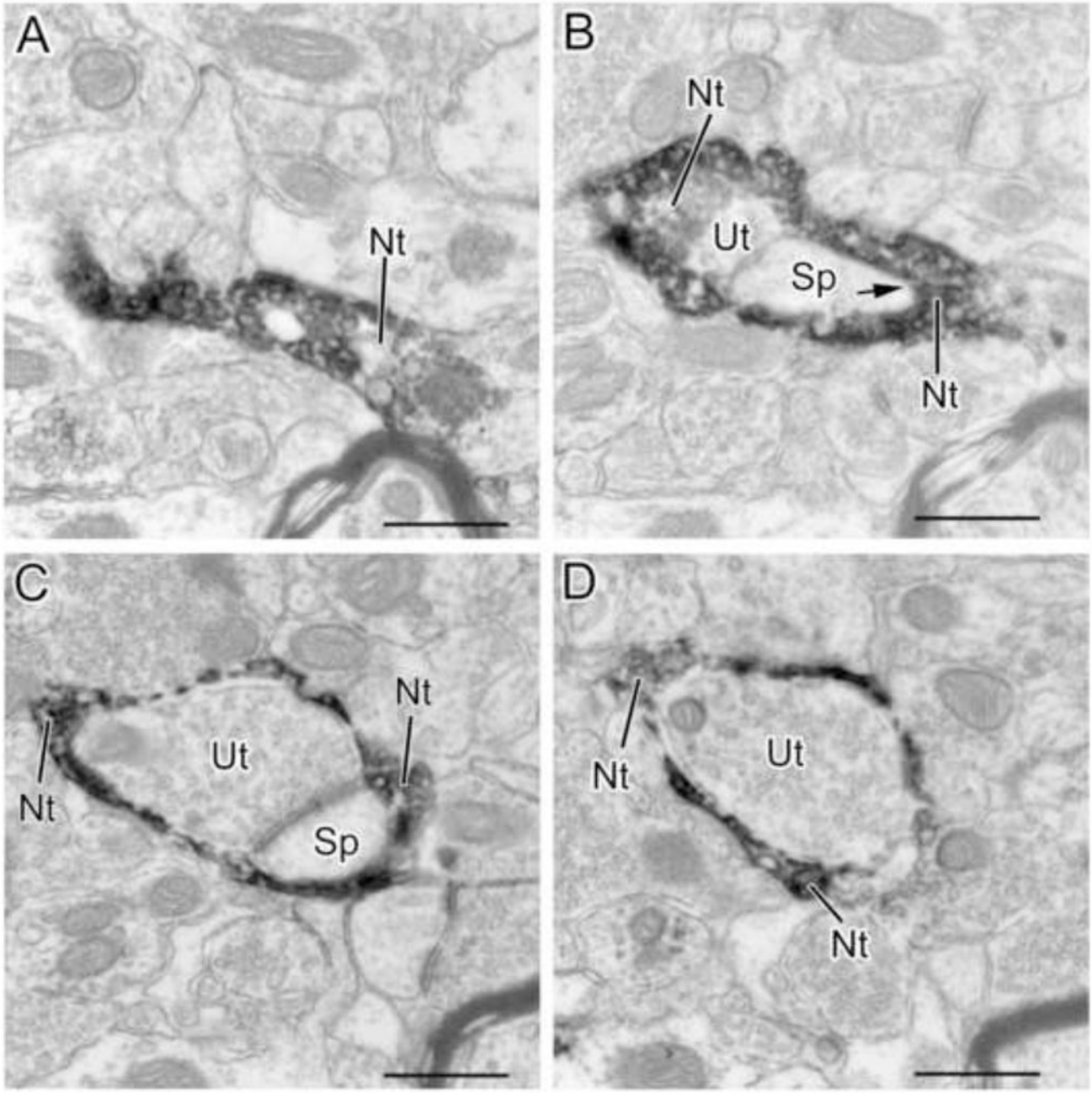

Fig. 8.

Four sections in sequential order (A–D) from a series of sections through an NET+ axon terminal (Nt) that envelops a synapse formed by an unlabeled axon terminal (Ut) and its postsynaptic spine (Sp). The NET+ terminal appears to form a synapse with the spine in B (arrow). A–D are the 1st, 4th, 8th and 12th sections, respectively, from a 13 section series. Scale bars = 500 nm.

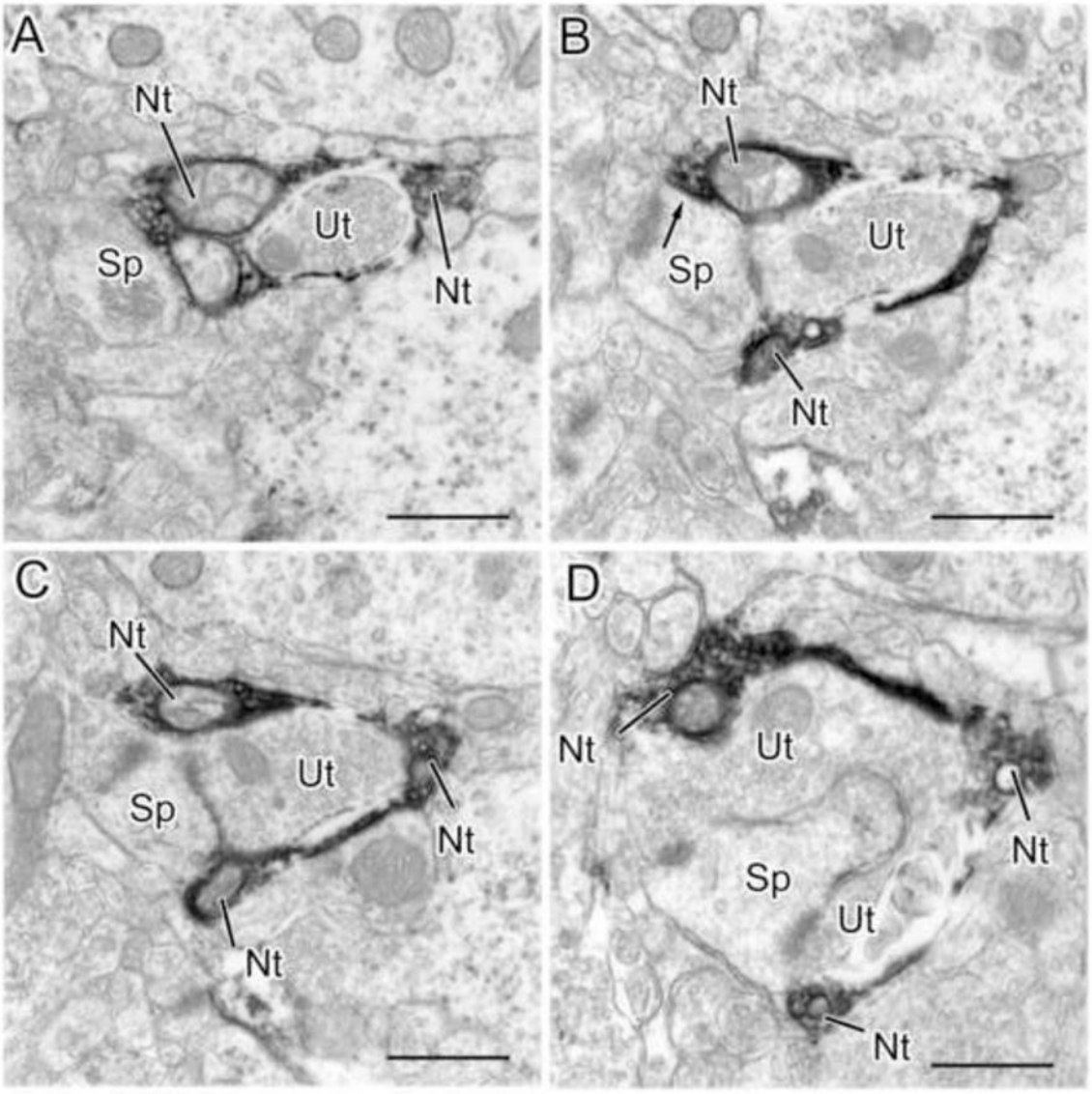

Fig. 9.

Four sections in sequential order (A–D) from a series of sections through an NET+ axon terminal (Nt in A) that envelops a synapse formed by an unlabeled axon terminal (Ut) and its postsynaptic spine (Sp). The NET+ terminal appears to form a synapse with the spine in B (arrow). A–D are the 2nd, 6th, 8th and 12th sections, respectively, from a 12 section series. Scale bars = 500 nm.

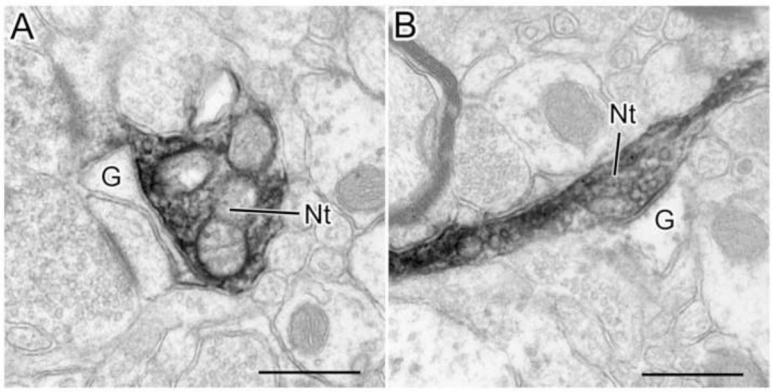

Fig. 10.

NET+ terminals (Nt) form appositions with astrocytic glial processes (G). A) An NET+ (Nt) terminal forms a broad apposition with an astrocytic process (G). The apposed membranes are fairly parallel and there appears to be dense material in the intervening cleft (especially along the lower portion). In contrast, the spaces surrounding other portions of the NET+ terminal are clear. Although somewhat obscured by the DAB reaction product, there are several synaptic vesicles adjacent to the membrane of the NET+ terminal that apposes the astrocyte. B) An NET+ terminal (Nt) forms a contact with an astrocytic process (G) that has several characteristics of a synapse. Note the parallel membrane thickenings and the dense material in the cleft (including cross bridges). Scale bars = 500 nm.

Table 1

Postsynaptic targets of NET+ terminals in the BLa.

	CaMK+ Somata	CaMK+ LD	CaMK+ SD	Spines	Unlabeled Somata	Unlabeled LD	Unlabeled SD
Symmetrical NET synapses	1	7	13	11	1	0	4
Asymmetrical NET synapses	0	1	2	3	0	1	1
Total NET synapses	1	8	15	14	1	1	5

LD, large dendrite (>1μm); SD, small dendrite (<1μm)